PROBABILISTIC ASSESSMENT OF THE SEISMIC VULNERABILITY OF REINFORCED CONCRETE FRAME BUILDINGS IN CANADA

L. Lin[1], N. Naumoski[2], S. Foo[3] and M. Saatcioglu[4]

[1] *Graduate research assistant, Dept. of Civil Engineering, University of Ottawa, Ottawa, Canada*
Email: llin089@gmail.com
[2] *Adjunct professor, Dept. of Civil Engineering, University of Ottawa, Ottawa, Canada*
E-mail: Nove.Naumoski@pwgsc.gc.ca
[3] *Risk specialist, Public Works and Government Services Canada, Gatineau, Quebec, Canada*
Email: Simon.Foo@pwgsc.gc.ca
[4] *Professor, Dept. of Civil Engineering, University of Ottawa, Ottawa, Canada*
Email: Murat.Saatcioglu@uottawa.ca

ABSTRACT:

This paper describes results from a study on the seismic vulnerability of three reinforced concrete frame buildings designed for Vancouver, Canada. The buildings included a 4-storey, a 10-storey, and a 16-storey building, that can be considered typical of low, intermediate, and high rise buildings respectively. The buildings were designed in accordance with the National Building Code of Canada. The seismic excitations used in the analyses were represented by a set of 80 ground motion records. The response parameter considered in this study is the maximum interstorey drift obtained from nonlinear dynamic analysis of the frames. The intensity of the seismic excitations is represented by the spectral acceleration at the fundamental structural period of the frames. The assessment of the seismic vulnerability is based on the consideration of the mean annual frequencies of exceeding selected drift levels, i.e., the drift hazard curves. The computation of the drift hazard curves was conducted using probabilistic seismic demand analysis.

KEYWORDS: reinforced concrete, building, interstorey drift, seismic, hazard, analysis.

1. INTRODUCTION

Seismic motions and resulting responses of structures due to such motions are probabilistic in nature, and therefore, a probabilistic approach needs to be used for the assessment of the seismic behaviour of structures due to future earthquakes. Probabilistic considerations have been already utilised in the new approach for the seismic assessment of existing structures and the design of new structures, known as the Performance-Based Earthquake Engineering (PBEE) (Cornell and Krawinkler 2000). An important phase of PBEE is the Probabilistic Seismic Demand Analysis (PSDA). The goal of PSDA for a given structure is to determine the mean annual frequencies of exceeding specified levels of structural response due to future earthquakes, i.e., to determine the response hazard curve. This is done by combining the seismic hazard at the location of the structure considered, and the response of the structure subjected to a set of earthquake motions scaled to a range of intensity levels.

In this study, the structural response was represented by the maximum interstorey drift. The seismic vulnerability was assessed based on the drift hazard curves for the frames of the buildings, computed using PSDA. Since the damage to buildings can be related to the interstorey drift (e.g., ASCE 2000), the drift hazard curves can be used to estimate the damage and consequently the financial loss due to earthquake motions.

2. DESCRIPTION OF BUILDINGS

Three reinforced concrete frame buildings were used in this study (Fig. 1). The buildings are for office use and are located in Vancouver, which is in a high seismic hazard zone (NRCC 2005). The buildings are the same in plan but have different heights. As shown in Fig. 1, the buildings include a 4-storey, a 10-storey, and a 16-storey building, which are considered representative of low-rise, medium-rise and high-rise buildings respectively.

The plan of each building is 27.0 m x 63.0 m. The storey heights are 3.65 m. The lateral load resisting system consists of moment-resisting reinforced concrete frames in both the longitudinal and the transverse directions. There are four frames in the longitudinal direction and eight frames in the transverse direction. The distance between both the longitudinal and the transverse frames is 9.0 m. Secondary beams between the longitudinal frames are used at the floor levels in order to reduce the depth of the floor slabs. The floor system consists of a one-way slab spanning in the transverse direction.

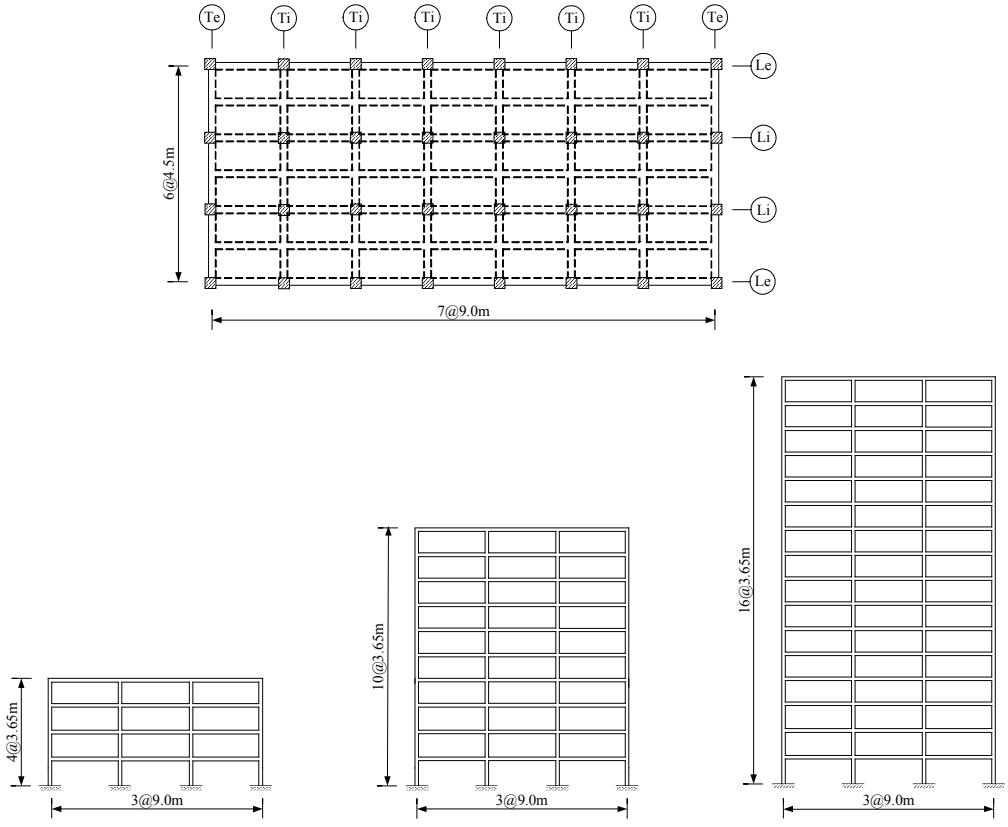

Figure 1 Plan of floors and elevations of transverse frames of the buildings.

3. DESIGN OF FRAMES

In this study, only the interior transverse frames of the buildings were considered (i.e., frames *Ti* in Fig. 1). For ease of discussing, the 4-storey, the 10-storey, and the 16-storey frames are referred to as the 4S, the 10S, and the 16S frames respectively. The frames were designed as *ductile* reinforced concrete frames. The gravity and the seismic loads were determined according to the 2005 edition of the National Building Code of Canada (NBCC) (NRCC 2005). Each frame was treated as an individual structural unit with its own gravity and seismic loads. 'Reference' ground conditions, represented by site class C in NBCC, were assumed at the building locations. The member forces for use in the design were determined by elastic analyses of the frames subjected to the combinations of gravity and seismic loads as specified in NBCC. Compressive strength of concrete f_c' =

30 MPa, and yield strength of reinforcement f_y = 400 MPa were used in the design. The dimensions of the columns and beams, and the reinforcement obtained from the design are given in Lin (2008).

4. MODELLING OF FRAMES FOR DYNAMIC ANALYSIS

The computer program RUAUMOKO (Carr 2004) was used for the inelastic dynamic analysis of the frames subjected to seismic motions. It is a two-dimensional (2-D) analysis program, which provides a wide range of modelling options. For each frame, a 2-D inelastic model was developed for use in RUAUMOKO. The beams and columns were modelled by a 'beam-column' element, which is represented by a single component flexural spring. Inelastic deformations are assumed to occur at the ends of the element where plastic hinges can be formed. The effects of axial deformations in beams are neglected. Axial deformations are considered for columns, but no interaction between bending moment and axial load is taken into account. A trilinear hysteretic model was selected for the columns, and a bilinear (modified Takeda) model was selected for the beams from the models available in RUAUMOKO. Both models take into account the degradation of the stiffness during nonlinear response. The first mode periods obtained by RUAUMOKO for the 4S, the 10S, and the 16S frames are 0.94 s, 1.96 s, and 2.75 s respectively.

5. SEISMIC EXCITATIONS

Ground motion records from earthquakes in the Vancouver region would be the most suitable for the analysis of the frames considered in this study. Since such records are not available, recorded ground motions from earthquakes in California were selected. It is commonly believed that the characteristics of crustal earthquakes that might occur in the Vancouver region are similar to those of California earthquakes.

For the purpose of this study, 80 earthquake records were selected from the strong motion database of the Pacific Earthquake Engineering Research (PEER) Center. All the records were obtained at sites class C (shear wave velocities between 360 m/s and 750 m/s), which was assumed in the design of the frames. The records were obtained from 22 earthquakes with magnitudes ranging from 5.8 to 7.3, and at distances ranging from 10 km to 109 km. The peak ground accelerations of the records are between 0.04 g and 0.36 g. A detailed discussion of the characteristics of the records can be found in Lin (2008).

6. PROBABILISTIC SEISMIC DEMAND ANALYSIS OF THE FRAMES

6.1. Formulation of Demand Hazard Curve

The goal of probabilistic seismic demand analysis (PSDA) is to compute the mean annual frequencies of exceeding given levels of structural response due to future earthquakes. This is done by integrating probabilistic structural response over all potential levels of ground motion intensity. Following PEER practice, the structural response demand in PSDA is quantified using an engineering demand parameter (*EDP*), and the intensity of the seismic motions is represented by an intensity measure (*IM*). Using this terminology, the mean annual frequency of exceeding a given *EDP* value *edp*, designated $\lambda_{EDP}(edp)$, is calculated as (Baker and Cornell 2005):

$$\lambda_{EDP}(edp) = \int_{im} P(EDP > edp \mid IM = im) \cdot \left| \frac{d\lambda_{IM}(im)}{d(im)} \right| \cdot d(im) \tag{6.1}$$

$\lambda_{EDP}(edp)$ is also referred to as the demand hazard curve. In this equation, the term $P(EDP>edp|IM=im)$ is the conditional probability of exceeding a specified *EDP* level *edp*, given a level of $IM=im$. The term $\lambda_{IM}(im)$ is the mean annual frequency of exceeding a given *IM* value *im* (this is commonly referred to as the ground motion or seismic hazard curve).

It is seen in Equation (6.1) that *EDP* and *IM* are required in order to conduct PSDA. In this study, the maximum interstorey drift (*IDR*) over the height of the frames is used as *EDP*. The maximum *IDR* is a 'global' response parameter and is used as an indicator for damage to structures due to earthquake motions (e.g., ASCE 2000). The *IM* was represented by the elastic spectral acceleration at the fundamental structural period T_1 ($Sa(T_1)$), which is currently the most used *IM*. Using *IDR* as *EDP*, and $Sa(T_1)$ as *IM*, Equation (6.1) can be written as follows:

$$\lambda_{IDR}(idr) = \int_{sa} P(IDR > idr \mid Sa(T_1) = sa) \cdot \left| \frac{d\lambda_{Sa(T_1)}(sa)}{d(sa)} \right| \cdot d(sa) \tag{6.2}$$

6.2. Analysis Method

As seen in Equation (6.2), the determination of the drift hazard curve, $\lambda_{IDR}(idr)$, for a given structure involves computations of: (i) the maximum *IDR*s of the structure for different $Sa(T_1)$ levels *sa*, (ii) the conditional probabilities $P(IDR>idr|Sa(T_1)=sa)$, and (iii) the spectral acceleration hazard curve $\lambda_{Sa(T_1)}(sa)$ for the location of the structure. The numerical procedures used in the analysis and the results obtained for the frames are described in the next sub-sections.

*6.2.1 Maximum IDR*s

The responses of the frame models were computed using nonlinear time history analyses for excitation motions represented by the selected set of 80 records. To determine the maximum *IDR*s due to ground motions with different intensities, the records were scaled to a range of $Sa(T_1)$ intensity levels. Note that T_1=0.94 s for the 4S frame, 1.96 s for the 10S frame, and 2.75 s for the 16S frame. In total 16 levels were used for the 4S frame, and 14 levels for each of the 10S and the 16S frames. Figure 2 shows the computed maximum *IDR*s versus the intensity levels Sa(T_1). *IDR* values of the order of 15% and above can be seen for the highest $Sa(T_1)$ levels used in the analysis. Certainly, such large *IDR*s cannot be resisted by the frames, i.e., the frames would collapse when their *ultimate* drift capacities (i.e., collapse drift limits) are exceeded. It is important for this study to know how many records produce collapse at a given $Sa(T_1)$ intensity. Since the program RUAUMOKO does not identify the collapse, an estimate of the ultimate drift capacities of the frames is needed in order to determine which records cause collapse. In this study, the collapse was defined to occur if the *IDR* obtained from the dynamic analysis exceeds 5%. The selection of the value of 5% as ultimate drift for the frames analysed in this study is discussed in detail in Lin (2008).

6.2.2 Calculation of the probability P(IDR>idr|Sa(T1)=sa)

To calculate the probability $P(IDR>idr|Sa(T_1)=sa)$, one should consider both the *IDR*s that are below the 5% ultimate drift (referred to as the non-collapse *IDR*s) and those that exceed the ultimate drift (referred to as the collapses) (Fig. 2). Assuming lognormal distribution of the non-collapse *IDR*s at each level $Sa(T_1)=sa$, the conditional probability for the *non-collapse IDR*s can be expressed as:

$$P(IDR > idr \mid Sa(T_1) = sa, nocollapse) = 1 - \Phi\left(\frac{(\ln idr \mid Sa(T_1) = sa) - \mu_{\ln IDR|Sa(T_1)=sa}}{\sigma_{\ln IDR|Sa(T_1)=sa}} \right) \tag{6.3}$$

where $\Phi(\cdot)$ denotes the standard normal cumulative distribution function. In this equation, $\mu_{\ln IDR|Sa(T_1)=sa}$ and $\sigma_{\ln IDR|Sa(T_1)=sa}$ represent respectively the mean and the standard deviation of the natural logarithms of the *IDR*s at intensity level $Sa(T_1)=sa$.

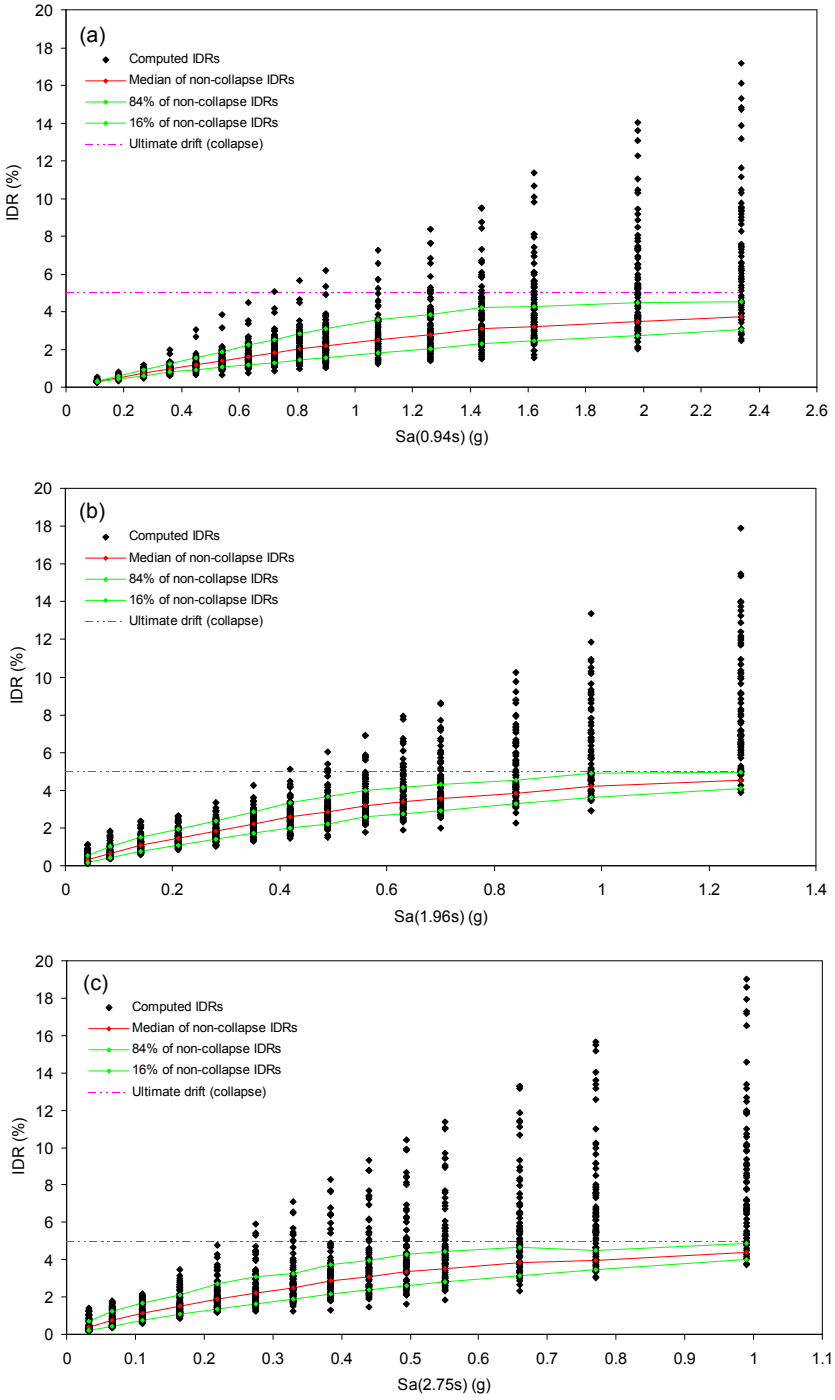

Figure 2 Computed maximum *IDR*s for records scaled to spectral acceleration at the first mode period, $Sa(T_1)$: (a) for the 4S frame, (b) for the 10S frame, and (c) for the 16S frame.

The calculation of the probability of *collapse* was done as suggested by Baker and Cornell (2005). First, the discrete probability that collapse (C) has occurred at a given $Sa(T_1)=sa$ was determined using the equation:

$$P(C|Sa(T_1)=sa) = \frac{\text{number of collapses}}{\text{total number of responses}} \tag{6.4}$$

As indicated by Equation (6.4), the calculation of the collapse probabilities $P(C|Sa(T_1)=sa)$ for each frame was simply done by counting the collapses for each $Sa(T_1)=sa$, and expressing these as a fraction of the total number of responses of 80. The computed discrete probabilities for the 4S, the 10S, and the 16S frames are shown by symbols in Figure 3. Since analytical expressions for the collapse prediction are required for PSDA, curves were fitted (shown in Fig. 3) assuming lognormal distribution of the collapses.

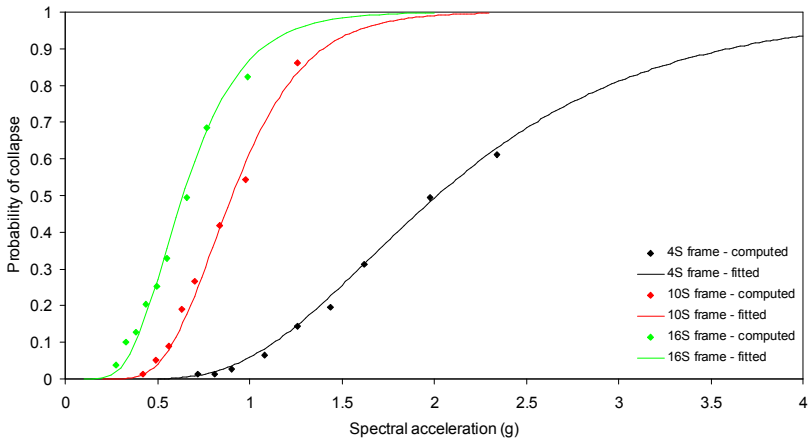

Figure 3 Computed probability of collapse (denoted by symbols) and fitted probability of collapse distributions for the 4S, the 10S, and the 16S frames.

The probabilities of the non-collapse and the collapse results defined above were combined using the total probability theorem. The probability that *IDR* exceeds a specified value *idr* for a given $Sa(T_1)=sa$ is expressed as:

$$P(IDR > idr \mid Sa(T_1) = sa) = P(C \mid Sa(T_1) = sa) + \left[1 - P(C \mid Sa(T_1) = sa)\right] \cdot \left[1 - \Phi\left(\frac{\ln idr - \mu_{\ln IDR|Sa(T_1)=sa}}{\sigma_{\ln IDR|Sa(T_1)=sa}}\right)\right] \quad (6.5)$$

6.2.3 Seismic hazard curves, $\lambda_{Sa(T_1)}(sa)$

In general, the seismic hazard curve $\lambda_{Sa(T_1)}(sa)$ for a given site and structural period T_1 is computed using probabilistic seismic hazard analysis (PSHA). PSHA combines the hazard contributions of the seismic source zones affecting the site. This is done by considering the seismic activities of the zones and using the attenuation relation for $Sa(T_1)$ (Adams and Halchuk 2003).

For this study, seismic hazard curves for Vancouver were determined for 5% damped *Sa* for periods of 0.94 s, 1.96 s, and 2.75 s, which are the fundamental periods of the 4S, the 10S, and the 16S frame respectively (Fig. 4). It can be seen in Fig. 4 that the mean annual frequencies of exceeding the spectral accelerations for period of 0.94 s are larger than those for periods of 1.96 s and 2.75 s. This is expected because larger spectral accelerations are normally associated with shorter periods (except for very short periods, e.g., below 0.2 s).

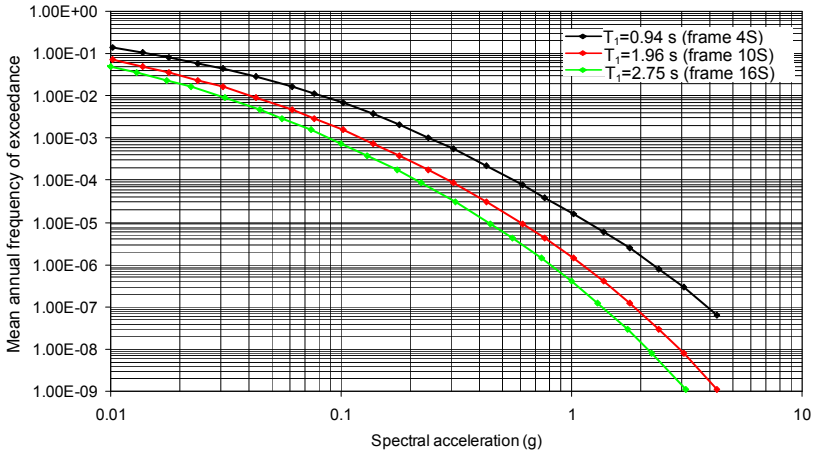

Figure 4 Seismic hazard curves for Vancouver expressed in terms of spectral acceleration at the fundamental periods of the 4S, the 10S, and the 16S frames of 0.94 s, 1.96 s, and 2.75 s respectively.

6.2.4 Drift hazard curves for the frames, $\lambda_{IDR}(idr)$

Having determined the probability distributions $P(IDR>idr|Sa(T_1)=sa)$ for the frames, and the seismic hazard curves $\lambda_{Sa(T_1)}(sa)$ for the site, the mean annual frequencies of *IDR* exceeding a set of *idr* values, denoted $\lambda_{IDR}(idr)$, can be computed using Equation (6.2). The function $\lambda_{IDR}(idr)$ is referred to as the drift hazard curve. In this study, numerical integration was used to determine the drift hazard curves, making use of the discrete summation approximation. Values for *sa* ranging between 0.01g and 4.0 g, at a step of 0.01g were used in the numerical integration. Mean annual frequencies (MAF) of exceedance were computed for selected drift values between 0.27% (1.0 cm) and 5.0% (18.25 cm). Note that the drift of 5.0% corresponds to collapse of the frames, as discussed above.

The computed drift hazard curves are shown in Fig. 5. It is seen that the largest MAF values are for the 16S frame, and the smallest values are for the 4S frame within the entire drift range considered (i.e., between drifts of 0.27% and 5.0%). The MAF values for the 10S frame are in between those for the 16S and the 4S frames. This indicates that among the three frames, the most vulnerable is the 16S frame and the least vulnerable is the 4S frame.

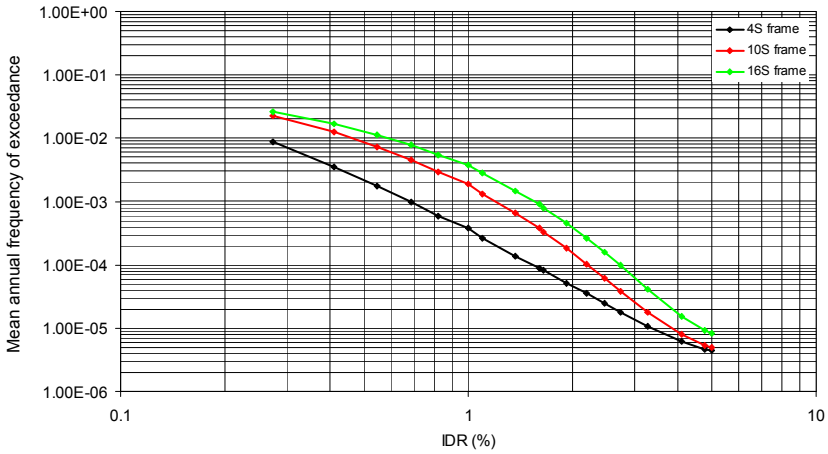

Figure 5 Drift hazard curves for the 4S, the 10S, and the 16S frames.

7. DISCUSSION AND CONCLUSIONS

Three reinforced concrete frames (4-, 10-, and 16-storey high) designed for Vancouver were used in this study. Eighty records representative of seismic conditions in the Vancouver region were used as excitation motions. The seismic vulnerability of the frames was assessed using probabilistic seismic demand analysis (PSDA). PSDA combines the seismic hazard at the location and the seismic response of the frames subjected to the selected motions. The maximum interstorey drift obtained from nonlinear time history analysis of the frames was considered as a response parameter, and the spectral acceleration at the fundamental structural period was considered as an intensity measure in the PSDA. The final results from the PSDA were the drift hazard curves, which represent the mean annual frequencies of exceeding specified drift values. While the results are not presented in this paper (because of space limitation), preliminary analyses were conducted to investigate the effects of the number of records on the drift hazard curves. This was done by computing the drift hazard curves for 40 records that were randomly selected from the set of 80 records.

The results showed that among the three frames analysed in this study, the most vulnerable is the 16-storey (i.e., the high rise) frame, and the least vulnerable is the 4-storey (i.e., the low rise frame). The drift hazard curves obtained for the frames can be used for the assessment of damage to the frames, and consequently for the estimation of losses due to future earthquakes.

Preliminary analysis showed that the drift hazard curves are quite sensitive to the number of records used in the PSDA, especially for larger drift values. This subject, however, is still under investigation by these authors.

REFERENCES

Adams, J., and Halchuk, S. (2003). Fourth generation seismic hazard maps of Canada: Values for over 650 Canadian localities intended for the 2005 National Building Code of Canada. Open File Report 4459, Geological Survey of Canada, Ottawa, Ont., 155 p.

ASCE. (2000). Prestandard and commentary for the seismic rehabilitation of buildings. Report FEMA 356, American Society of Civil Engineers, Reston, Virginia.

Baker, J.W., and Cornell, C.A. (2005). A vector-valued ground motion intensity measure consisting of spectral acceleration and epsilon. *Earthquake Engineering and Structural Dynamics*, 34: 1193-1217.

Carr, A.J. (2004). RUAUMOKO – Inelastic dynamic analysis program. Department of Civil Engineering, University of Canterbury, Christchurch, New Zealand.

Cornell, C.A., and Krawinkler, H. 2000. Progress and challenges in seismic performance assessment. PEER Center News, 3(2), 4 p.

Lin, L. (2008). Development of improved intensity measures for probabilistic seismic demand analysis. PhD. thesis, Submitted, Department of Civil Engineering, University of Ottawa, Ottawa, Ont., Canada.

NRCC. (2005). National Building Code of Canada 2005. Institute for Research in Construction, National Research Council of Canada, Ottawa, Ont., Canada.